Electric Fatigue of Ceramic–Polymer Composite Film Under Cyclic Electric Field

F. Fang,[1] W. Yang,[1,2] M. Z. Zhang,[1] Z. Wang[1]

[1]*Failure Mechanics Laboratory, School of Aerospace, Tsinghua University, Beijing 100084, China*
[2]*The University Office, Zhejiang University, Hangzhou 310058, China*

Received 8 May 2008; accepted 18 August 2008
DOI 10.1002/app.29120
Published online 17 October 2008 in Wiley InterScience (www.interscience.wiley.com).

ABSTRACT: Electric fatigue under cyclic electric loading was characterized for 0–3 composite film with particles of barium titanate dispersed in poly(vinylidene fluoride-trifluoroethylene) copolymer matrix. The data reveal that both remanant polarization and coercive field decrease as the cycle number increases. Scanning electron microscope observation and X-ray diffraction analysis were carried out to examine the morphology and microstructure change during the electric field cycling. On cyclic electric field, large quantities of flaw-like defects occur and the crystallites grow in size, leading to reduction of interfacial layers between the crystalline and amorphous regions. The relationship between the microstructure evolution and the polarization behavior is discussed. © 2008 Wiley Periodicals, Inc. J Appl Polym Sci 111: 1105–1109, 2009

Key words: electric fatigue; ceramic–polymer composite; ferroelectric film; P(VDF-TrFE); polarization degradation

INTRODUCTION

Ferroelectric polymer based 0–3 composite films, which are formed by suspending 0-dimensional ceramic powders into a 3-dimensional continuative polymer matrix, have attracted much attention for their promising applications such as capacitors, embedded sensors, and electric energy storage devices.[1–6] The created composites combine the advantages of ceramics and polymers and present a novel type of material which is easy to process, with high dielectric constant, high electromechanical efficiency, and high breakdown strength.[1,7–10] The ceramic fillers used in the composites are usually ferroelectrics with high dielectric constant, such as calcium or samarium and magnesium modified lead titanium,[2,5–8,11] lead zirconate titanate,[3,6] lead magnesium niobate (PMN-PT),[9] and barium titanate ($BaTiO_3$).[10] The polymer host material used includes perfluorocyclobutene homopolymer,[10] polyetherketonketone (PEKK),[2,5] poly(vinylidene fluoride) (PVDF),[3] poly(vinylidene fluoride-trifluoroethylene) (P(VDF-TrFE)),[7,8,11] and epoxy,[7,8,11] etc. Among ferroelectric polymers, copolymers of P(VDF-TrFE) are the best known and exhibit the best ferroelectric and piezoelectric performances.[12–15] For instance, it was reported that a very large electric-field induced strain response, as high as 5%, with low hysteresis can be obtained for electron irradiated P(VDF-TrFE) copolymers which is very attractive for many electromechanical applications.[13–15]

For ferroelectric ceramics and single crystals, it is well known that its polarization hysteresis exhibits a fatigue behavior, which reflects the degradation of polarization with electric cycles and limits the application of these materials. However, the fatigue behavior of the ferroelectric polymers and the ceramic–polymer composites is rarely investigated. It was recently reported that for the directly annealed P(VDF-TrFE) 68/32 copolymer films, the remanent polarization (P_r) decreased whereas the coercive field (E_c) increased as the field cycles. For the stretched films, both P_r and E_c decreased as the cycle number increased.[16] In this article, electric fatigue behavior of $BaTiO_3$-P(VDF-TrFE) 0–3 composite film is reported. Scanning electron microscope observation and X-ray diffraction analysis were carried out to examine the morphology and microstructure change during the electric field cycling. The relationship between the microstructure evolution and the polarization behavior was discussed.

EXPERIMENTAL

The composite films were prepared by solution-casting method which employs a $BaTiO_3$ powder–polymer dispersion. P(VDF-TrFE) 68/32 mol % obtained from Solvay Company (Belgium) was used as the

Correspondence to: F. Fang (fangf@mail.tsinghua.edu.cn).
Contract grant sponsor: National Natural Science Foundation of China and National Basic Research Program of China; contract grant number: 2004CB619304.

polymer host material. When preparing the solution, P(VDF-TrFE) powders were first dissolved using dimethylformamide as solvent. Then, $BaTiO_3$ powders (purity 99.5%, with average size of 50–60 nm) were added to the polymer solution to achieve a weight filling fraction of 10% (wt ($BaTiO_3$)/wt (P(VDF-TrFE) + $BaTiO_3$), or a volume fraction of 3.4%. After the dispersion was stirred carefully to achieve a homogeneous mixture, it was poured onto the clean glass plates and heated at 70°C for more than 12 h to remove the solvent. The dried films were carefully peeled off from the glass plates and were later annealed in a vacuum oven at 135°C for 2 h. The composite films obtained have thicknesses ranging from 35 to 45 μm.

For polarization characterization, the films were sputtered with gold on both surfaces as electrodes. The polarization hysteresis (*P–E* curve) was measured using the Sawyer-Tower technique. The applied ac field had a sinusoidal waveform, with a fixed frequency of 10 Hz. It was supplied from a voltage amplifier (Trek-610E-K-CE, by Trek, USA) that amplified its input from a function generator (TTI-TG1010, by Thurlby Thandar Instruments, UK). In the experiments, we first obtained the polarization hysteresis loops at different field magnitude which was from 15 MV/m to 75 MV/m with an interval of 10 MV/m. Then, we chose a field magnitude at which a well shaped polarization loop could be obtained. Here, the field magnitude of 60 MV/m was chosen, and the P–E curves were measured continuously and recorded at different cycle numbers. Three to five film samples were used to obtain the polarization loop. During the P–E curve measurements, the samples were immersed in a silicon oil to avoid arcing.

The morphology and microstructure of the samples were characterized using XRD and SEM. Samples before and after 50,000 electric cycles were examined using a Hitachi S-4500 field emission scanning electron microscope (FE-SEM). X-ray experiments were conducted in a reflection mode by using a MX18A-HF X X-ray diffractometer with CuKα radiation (wavelength 0.154 nm), operated at 40 kV and 30 mA.

RESULTS

With a constant ac field, the polarization–electric field (P–E) curve changes with the cycle numbers in a monotonic trend. Figure 1(a) shows polarization hysteresis loops for the composite film at the field of 60 mV/m. For a fresh sample, the value of P_r, P_s, and E_c are 25.6 mC/m^2, 35.1 mC/m^2, and 38.8 MV/m. The data shown in Figure 1(b) are cycle dependence of P_r, P_s, and E_c for the composite film. All the data were obtained by averaging the corresponding plus and minus values. As the cycle number

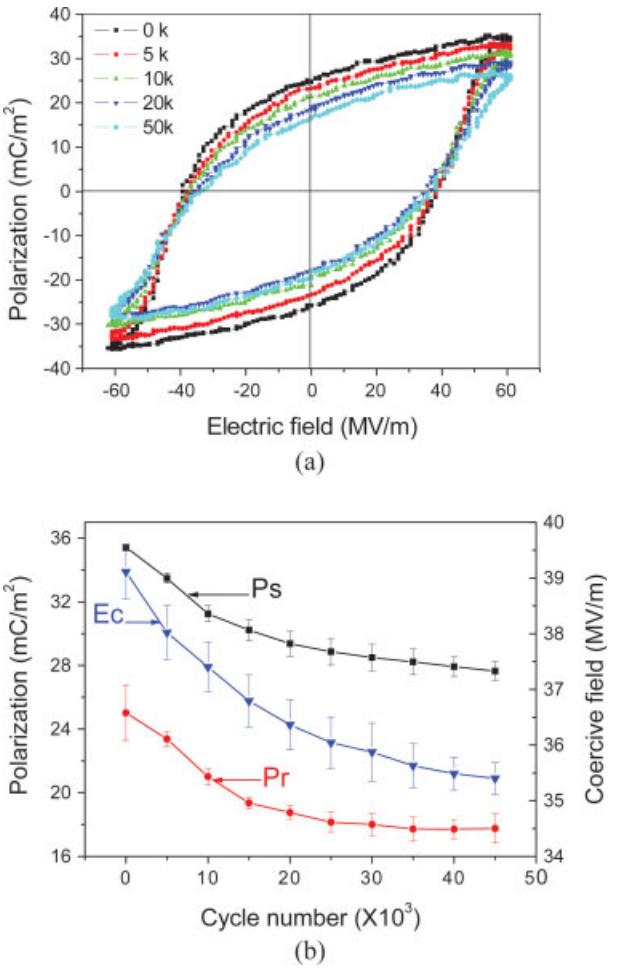

Figure 1 (a) Polarization hysteresis loops and (b) P_r, P_s, and E_c versus number of cycles for the composite film at a field magnitude of 60 mV/m. [Color figure can be viewed in the online issue, which is available at www.interscience.wiley.com.]

increases, both P_r (or P_s) and E_c decrease, and P_r reduces 30% of its original value after 50,000 electric cycles. For the change of minus and plus E_c with the cycle number, $-E_c$ shows this trend apparently while $+E_c$ first show this trend but later it shows the opposite trend after approximately 20,000 cycles.

Shown in Figure 2 is the SEM morphology change for the composite film before and after electric cycling. It can be seen that the original undulant rod-like textures gradually level off and the crystallites gradually grow in size, leading to reduction of the interfacial areas between the amorphous and the crystalline regions. The average sizes in width of the rod-like textures are about 45 nm and 70 nm for initial and fatigued film, respectively.

It can also be seen that large amounts of flaw-like defects appear for the fatigued sample.

Figure 3 shows the X-ray diffraction (XRD) patterns for the composite film before and after the electric cycling. For the fresh sample, the peak which locates at

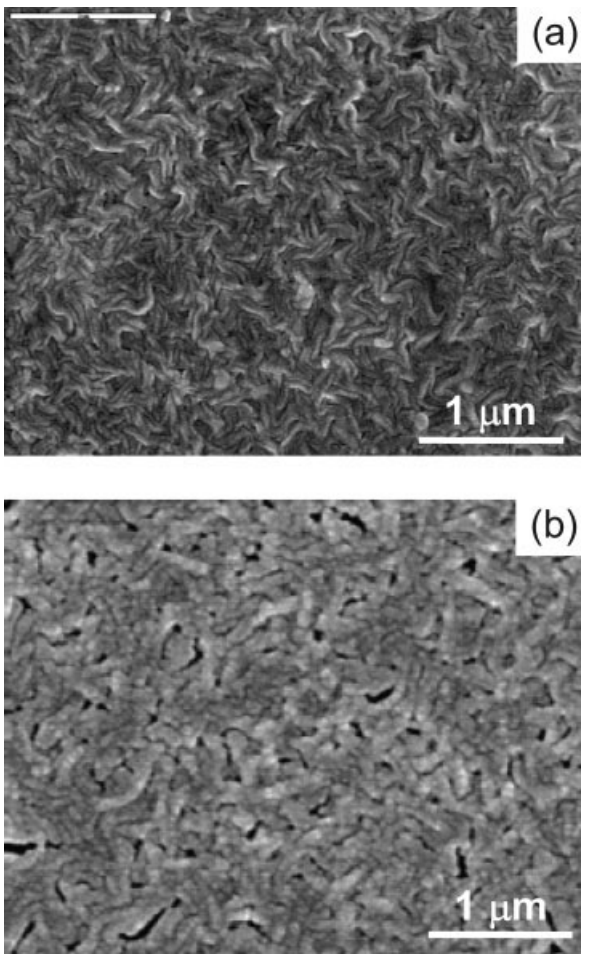

Figure 2 SEM micrographs showing surface morphology change for the compositer film: (a) initial state, (b) fatigued 50,000 cycles and broken. The applied electric field was in the film thickness direction. That is, the electric field was perpendicular to the surface.

$2\theta = 19.56$ is from the (110, 200) reflection of the crystalline β phase of the P(VDF-TrFE) copolymer. Another peak which locates at $2\theta = 22.15°$ for the fresh sample is from the (100) reflection of the $BaTiO_3$ phase. The peak positions for the fatigued sample move toward higher angle, with 2θ equals 19.82° for the β (110, 200) reflection, and 22.29° for the $BaTiO_3$ {001} reflection. The full width of half maximum of the (110, 200) reflection peak of the crystalline β phase is 0.525° and 0.495° for the fresh and fatigued sample, respectively. These indicate that the crystallites in the fatigued samples are of a structure with a smaller interchain spacing and the domains of the crystallites in the fatigued samples have a bigger size. The diffraction intensity for the {100} reflection of the $BaTiO_3$ phase does not change much.

DISCUSSION

In P(VDF-TrFE) copolymer, the fluorine and hydrogen atoms have different polarity and form a dipole with a dipole moment of $m = 7 \times 10^{-30}\ C \cdot m$ (Coulomb-meter).[17] P(VDF-TrFE) is a semicrystalline polymer, in which the crystallite (or the crystalline region) has folded chain structure embedded in the amorphous.[17] That is, the molecular chains fold back on themselves to form thin platelets called lamellae. The crystallites within the polymer are randomly oriented, and in each crystallite, the dipole moments are randomly oriented in a plane normal to the molecular chain axis. Polarization mainly comes from the crystalline phase on the applied electric field. Because of very small crystallite size, there are large quantities of interfacial layers between the crystalline and amorphous regions (abbreviated as crystallite/amorphous interfaces). Since molecular chains in the crystallite/amorphous interfaces are packed partially ordered, they may become ordered on the applied electric field and contribute toward the overall polarization, as it was previously reported by Li et al.[18,19]

When the P(VDF-TrFE) copolymer film is subjected to an electric field, the reorientation of the electric dipoles of a crystallite occurs through a 60°, rather than 180°, rotation model plus a small distortion (1%) of the lattice.[20,21] Its occurrence is due to the orthorhombic symmetry of the unit cell of β phase resulting from a small (1%) distortion of an underlying hexagonal primitive lattice.[20,21] The small change in crystal axis dimension that occurs in the 60°-rotational model would cause internal strains in the crystallites. Further, dipole reorientation would also cause the polymer chains to rotate and align preferably in the direction perpendicular to the applied electric field.[16] The rotation of the electric dipoles and molecular chains in the crystalline regions induce internal strain at the crystallite/amorphous interfaces. As a result, rod-like textures gradually level-off and the crystallites grow in size, as being observed by SEM morphologies for both the

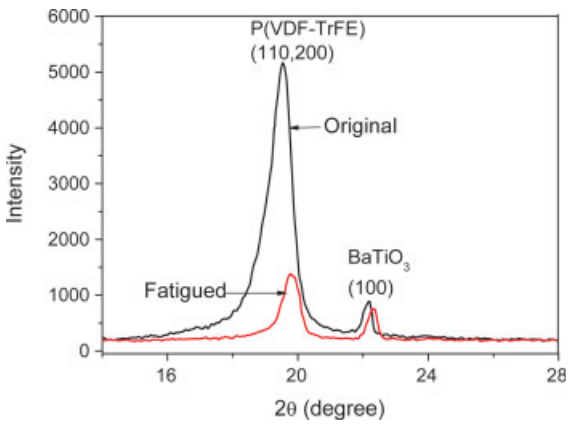

Figure 3 X-ray diffraction patterns for the composite films: initial state and electric fatigued (50,000 cycles). [Color figure can be viewed in the online issue, which is available at www.interscience.wiley.com.]

composite film (Fig. 2) and the P(VDF-TrFE) copolymer film.[16]

Compared with the pure P(VDF-TrFE) copolymer film, introduction of $BaTiO_3$ powder to the polymer matrix inhibits the crystallization, leading to lower crystallinity, and smaller average crystallite size. The average size in width for the BaTiO3/polymer composite film is 45 nm, whereas it is about 110 nm for the P(VDF-TrFE) 68/32 copolymer film.[16] The reduction of crystallinity for $BaTiO_3$/P(VDF-TrFE) film can be verified by the comparatively lower P_r value before electric cycling than that for the P(VDF-TrFE) copolymer film which is about 49.5 mC/m^2. On cyclic electric field, the interfaces between the ceramic powders and the polymer (abbreviated as BaTiO3/polymer interfaces) also suffer from the incompatible strain. As a result, flaw-like defects or microcavities occur at the interfaces, as evidenced by the SEM morphology shown in Figure 2(b).

For P(VDF-TrFE) copolymer, the prominent X-ray peak is from the (110, 200) reflection of the crystalline β phase. The peak intensity is mainly affected by the crystallinity and the ordering degree of the molecular chains. As for the hola background beneath the peak, it is mainly attributed from the amorphous phase. Further, large quantities of crystallites/amorphous interfaces where the polymer chains are packed partially ordered contribute to both the peak intensity and the hola background beneath the peak. It can be seen from Figure 3 that the (110, 200) peak intensity for the fatigued sample is much lower than that of the fresh sample, as well as the hola background. By referring to the SEM morphology change (Fig. 2), it can be inferred that after electric cycling, the crystallites grow in size, leading to decrease of the interfacial regions which contribute to both the peak intensity and the hola background.

On cyclic electric field, P_r decreases with the cycle number. The degradation of the polarization for P(VDF-TrFE) copolymer films is believed to be related with the pinning of electric dipoles to the electrodes and defect structures such as vacancies and pores.[22,23] For the $BaTiO_3$/P(VDF-TrFE) composite film, $BaTiO_3$ powders act as defects and cause pinning of electric dipoles. Furthermore, reduction of crystallite/amorphous interfaces on cyclic electric loading also leads to polarization degradation on cyclic electric field.

As it was previously reported, interfaces are possible nucleation sites for polarization switching and switching can be facilitated near the interfaces.[24] The introduction of $BaTiO_3$ ceramic powders to the polymer matrix causes more amorphous/crystallite and ceramic powder/polymer interfaces. Consequently, polarization switching is easier for the composite film. The initial E_c value is 38.8 mV/m for the composite film whereas it is 46.6 mV/m for the copolymer film. On cyclic electric loading, E_c decreases with the cycle number for the P(VDF-TrFE)/$BaTiO_3$ composite film, which is in contrary with most of the ferroelectric materials including ceramics, single crystals, and polymers. However, we previously reported that for the stretched P(VDF-TrFE) 68/32 copolymer film, which was prepared by stretching the solution cast film to 500% of its original length followed by vacuum annealing, E_c decrease with the cycle number.[16] For both the composite film and the stretched copolymer film, it is common that they have large quantities of flaw-like defects under cyclic electric loading. Therefore, it is inferred that the flaw-like defects can act as the nucleation sites for the polarization reversal. As a result, E_c decreases with the cycle number. For the different behavior of plus and minus E_c change with the cycle number, it is suggested due to the pinning of negative polarization charges to the electrodes, which was previously reported by Sakai et al. in Ref. 23 Therefore, the interaction between trapped negative charges and dipoles in ferroelectric polymers gradually makes the reversal of dipoles more difficult under a positive electric field. Consequently, $+E_c$ increases after a certain amount of cycle number as the result of competition between the effects caused by increasing of flaw-like defects and pinning of negative charges.

CONCLUSIONS

Investigations on the electric fatigue of $BaTiO_3$-P(VDF-TrFE) 0–3 composite films demonstrate that $\pm P_r$ (or $\pm P_s$) and $-E_c$ decrease with the cycle number, whereas $+E_c$ first shows this trend but later has an opposite trend after a certain amount of cycle number. Introduction of $BaTiO_3$ powders inhibits the polymer crystallization and consequently reduces the initial P_r (or P_s) and E_c. On cyclic electric field, rotation of polymer chains and electric dipoles causes incompatible strain between the polymer/$BaTiO_3$, and crystalline/amorphous interfaces. Consequently, large quantities of flaw-like defects occur which causes both P_r and E_c to decrease with the cycle number. The competition between the effects caused by increasing of flaw-like defects and pinning of negative charge causes $+E_c$ to first decrease then increase after a certain amount of field cycles.

References

1. Arbatti, M.; Shan, X. B.; Cheng, Z. Y. Adv Mater 2007, 19, 1369.
2. Pelaiz-Barranco, A.; Lopez-Noda, R. J Appl Phys 2007, 102, 114102.
3. Seema, A.; Dayas, K. R.; Varghese, J. M. J Appl Polym Sci 2007, 106, 146.

4. Calame, J. P. J Appl Phys 2006, 99, 084101.
5. Pelaiz-Barranco, A.; Marin-Franch, P. J Appl Phys 2005, 97, 034104.
6. Glushanin, S. V.; Topolov, V. Y. J Phys D: Appl Phys 2005, 38, 2460.
7. Marin-Franch, P.; Tunnicliffe, D. L.; Das-Gupta, D. K. Mat Res Innovat 2001, 4, 334.
8. Wenger, M. P.; Almeida, P. L.; Blanas, P.; Shuford, R. J.; Das-Gupta, D. K. Polym Eng Sci 1999, 39, 483.
9. Bai, Y.; Cheng, Z. Y.; Bharti, V.; Xu, H. S.; Zhang, Q. M. Appl Phys Lett 2000, 76, 3804.
10. Vrejoiu, I.; Pedarnig, J. D.; Dinescu, M.; Bauer-Gogonea, S.; Bauerle, D. Appl Phys A 2002, 74, 407.
11. Marra, S. P.; Ramesh, K. T.; Douglas, A. S. Compos Sci Technol 1999, 59, 2163.
12. Nalwa, H. S. Ferroelectric Polymers: Chemistry, Physics, and Applications; Marcel Dekker: New York, 1995.
13. Zhang, Q. M.; Bharti, V.; Zhao, X. Science 1998, 280, 2101.
14. Cheng, Z. Y.; Bharti, V.; Xu, T. B.; Xu, H.; Mai, T.; Zhang, Q. M. Sens Actuat A 2001, 90, 138.
15. Li, Z. M.; Arbatti, M. D.; Cheng, Z. Y. Macromolecules 2004, 37, 79.
16. Fang, F.; Yang, W.; Zhang, M. Z. J Appl Phys 2007, 101, 044902.
17. Furukawa, T. Adv Colloid Interface Sci 1997, 71–72, 183.
18. Li, Z. M.; Li, S. Q.; Cheng, Z. Y. J App Phys 2005, 97, 014102.
19. Li, Z. M.; Wang, Y.; Cheng, Z. Y. Appl Phys Lett 2006, 88, 062904.
20. Kepler, R. G.; Anderson, R. A. J Appl Phys 1978, 49, 1232.
21. Aharon, H. D.; Sluckin, T. J.; Taylor, P. L. Phys Rev B 1980, 21, 3700.
22. Limbong, A.; Guy, I.; Zheng, Z. J.; Afifuddin, A.; Tansley, T. Ferroelectrics 1999, 230, 363.
23. Sakai, S.; Date, M.; Furukawa, T. Jap J Appl Phys Part 1 2002, 41, 3822.
24. Gerra, G.; Tagantsev, A. K.; Setter, N. Phys Rev Lett 2005, 94, 107602.